Electrochimica Acta 195 (2016) 9–18

Contents lists available at ScienceDirect

Electrochimica Acta

journal homepage: www.elsevier.com/locate/electacta

Asymmetric Bilayer Muscles. Cooperative and Antagonist Actuation

Masaki Fuchiwaki[a], Jose G. Martinez[b], Toribio F. Otero[b,1,*]

[a] Kyushu Institute of Technology, Department of Mechanical Information Science and Technology, 680-4 Kawazu, Iizuka(Fukuoka) 820-8502, Japan
[b] Center for Electrochemistry and Intelligent Materials (CEMI), Universidad Politécnica de Cartagena (UPCT), Aulario II, E-30203 Cartagena, Spain

ARTICLE INFO

Article history:
Received 22 December 2015
Received in revised form 12 February 2016
Accepted 16 February 2016
Available online 24 February 2016

Keywords:
Conducting polymer
Asymmetric bilayer muscle
Cooperative actuation
Antagonist actuation

ABSTRACT

Thick films of polypyrrole-paraphenolsulfonic acid (PPy-HpPS), polypyrrole-dodecylbenzensulfonic acid (PPy-DBS) and a bilayer PPy-HpPS/PPy-DBS (asymmetric bilayer) were electrogenerated from aqueous solutions. Two bilayers: PPy-HpPS/tape and tape/PPyDBS were constructed. The angular displacement of those three bilayer muscles was characterized in NaCl aqueous solution by cyclic voltammetry and parallel video recording of the bending movement. The attained coulo-voltammetric (charge-potential), dynamo-voltammetric (angle-potential) and coulo-dynamic (charge-angle) responses until different cathodic potential limits were analyzed. The dynamo-voltammetric and coulo-dynamic responses from the PPy-HpPS/tape and tape/PPyDBS muscles inform about the reaction driven ionic exchanges in the two PPy films. Electrochemo-dynamical responses from the asymmetric PPy-HpPS/PPy-DBS bilayer muscles are explained using those reactions. Cooperative dynamic effects exist when both layers follow complementary reaction-driven volume changes (swelling/shrinking, or shrinking/swelling) due to complementary entrance/expulsion of ions. The cooperative amplitude of the angle described by the asymmetric bilayer muscle is one order of magnitude larger than those attained from each of the conducting polymer/tape bilayer muscles. Antagonist dynamic actuation occurs when the two films swell, or shrink, simultaneously originating narrower angular displacements. Improving cooperative actuation or eliminating antagonist actuation and creeping by suitable selection of polymers and electrolytes seem the way to get most efficient polymeric motors and industrial products.

1. Introduction

Films of conducting polymers exchange ions and solvent during electrochemical reactions for charge and osmotic balance [1–3]. Those reactive dense gels mimic, in its simplest expression (reactive macromolecules, ions, water and reaction-driven conformational movements of the conducting polymer chains) the intracellular matrix in cells. There reactions originate and support life and life functions [4]. Any biological cell is a complex chemical reactor in which most of the reactions cannot be described by nowadays-available chemical models. Those models were developed from reactions taking place in gaseous phase or in dilute solutions [5,6], quite far from the dense gel of the intracellular matrix where functional reactions occur.

Several biomimetic properties of the conducting polymer change with the polymer-counterion composition driven by the reaction. Each of those properties allow the development of a biomimetic reaction-driven device [1,2,7]. Among those devices, artificial muscles are transducers of the reaction-driven volume variations, required to lodge or expel balancing counterions and solvent, into macroscopic linear [8–16] or bending movements from bilayer or multi-layer structures [17–29]. Thus, bending artificial muscles can be considered as polymeric Faradaic motors translating reaction-driven ionic and aqueous exchanges into large angular movements. Thinking in the opposite direction artificial muscles can be considered as useful tools for the identification and quantification of different processes linked to the electrochemical reaction. They are being used to clarity and quantify ionic and aqueous exchanges [30,31], osmotic and electrosomotic processes [32], creeping effects [33] and any other mechanical or chemical influence on the electrochemical reaction of the constitutive conducting polymer. During actuation a progressive variation of both, inter and intra-molecular interactions (polymer-polymer, polymer-ions, polymer-solvent and solvent-ions) occur inside the CP film. Thus, by changing the solvent, or the salt, the reaction can move from driving cation exchanges to anion exchanges, and vice versa [34,35]. The muscle can be proposed as a tool to quantify the evolution of the intra-molecular forces in reactive gels (artificial or biological) during reactions [4]. Similar variations during parallel biological reactions in functional cells defines health or illness [6].

* Corresponding author. Tel.: +34 968 325519; fax: +34 968 325915.
E-mail address: toribio.fotero@upct.es (T.F. Otero).
[1] ISE member.

http://dx.doi.org/10.1016/j.electacta.2016.02.104

An electroactive material layer (conducting polymer, redox polymer, carbon nanotube, graphene, and so on) and a passive (from the electrochemical point of view) material layer (tape, plastic, metal, wood, and so on) constitute those bilayer muscles. The passive film, if essential to generate the transversal muscular stress gradient during actuation, consumes a fraction of the applied electrical energy to be bended. As a result the muscular energetic efficiency and the angular displacement, for the same consumed charge, decrease.

One of the strategies followed trying to eliminate those two adverse effects getting more robust and efficient polymeric motors is by using asymmetric bilayer muscles. Two layers of the same conducting polymer, here polypyrrole (PPy), constitute an asymmetric bilayer muscle. One PPy layer is expected to swell during oxidation by entrance of anions pushing the bending movement. The second PPy layer must shrink during oxidation (simultaneously) by expulsion of cations pulling the bending movement. Reverse ionic exchanges, volumetric changes and bending movements should occur during reduction of the asymmetric bilayer. On this way both films are simultaneously active and larger angular movements are expected by consumption of the same charge, or of the same energy, than using polypyrrole/tape bilayers.

Thus, for a good design of most efficient polymeric motors we must select two compatible conducting polymers: bilayers can be constructed by consecutive electrogeneration. The two layers should present asymmetric volume changes during reaction. For the first layer we have selected a polypyrrole blend electrogenerated in presence of the large dodecylbenzenesulfonic acid (HDBS), the second was generated in presence of the shorter paraphenolsulfonic acid (HpPS) [36]. The two organic ions, DBS and pPS, generate very compatible films giving a uniform interpenetrated bilayer.

Here we will explore the parallel electro-chemo-dynamical characterization of the asymmetric bilayer muscle (PPy-HpPS/PPy-DBS) and each of the PPy-HpPS/tape [37] or PPy-DBS/tape [38] bilayers muscles in NaCl aqueous solutions. The aim is to characterize the three selected bilayer muscles, identifying any reaction-driven effect as ionic exchanges or intermolecular interaction changes, cooperative and antagonist dynamic effects, creeping effects, and so on. Advantages and disadvantages of using asymmetric bilayer muscles for the development of industrial products will be discussed.

2. Experimental methods

Either chemicals, methodologies and video recording of the bending movement under electrochemical control have been described in a previous work [39].

2.1. Preparation of Polypyrrole-paraphenolsulfonic acid/tape (PPy-HpPS/tape) bilayer muscle

PPy-HpPS films were electrogenerated from 0.2 M pyrrole and 0.05 M HpPS aqueous solutions (50 mL). The working electrode was a stainless steel plate having 6.6 cm^2 of surface area. Two similar stainless steel electrodes were used as counterelectrodes CE, one by WE side at a distance of 1.0 cm in order to get a uniform electric field. The reference electrode was Ag/AgCl (3 M KCl) from Metrohm. Potentials in this work are referred to this electrode. A constant current density of 0.5 mA cm^{-2} was applied to the WE during 1 hour at 0 °C. After water rinsing the coated electrode was dried in air for 24 hours. The electrode borders were scrapped and two PPy-HpPS films were peeled off and weighed using a microbalance, 20 μm thick and 4.8 mg mass. Those freestanding films were cut into 20 mm × 1 mm strips. After determining its mass, each strip was attached under pressure to a double-sided tape from 3 M. A paint (Max Effect, MAXFACTOR) strip from 5.0 mm to 12.0 mm of the upper border avoids the direct contact between the electrolyte (by capillarity) and the metallic clamp that allows the electrical contact (Fig. 1a). The final bilayer muscle inside the solutions was 8 mm long.

2.2. Preparation of tape/Polypyrrole-dodecylbenzenesulfonic acid (PPy-DBS/tape) bilayer muscle

A similar procedure was used to electrogenerate on a stainless steel electrode a Polypyrrole-dodecylbenzenesulfonic acid (PPy-DBS) film from 0.15 M pyrrole and 0.25 M DBSA aqueous solution (50 mL). Two PPy-DBS film (one by side), 20 μm thick and 22 mg mass, were attained, cut in small pieces and attached to a tape getting the final tape/PPy-DBS bilayer.

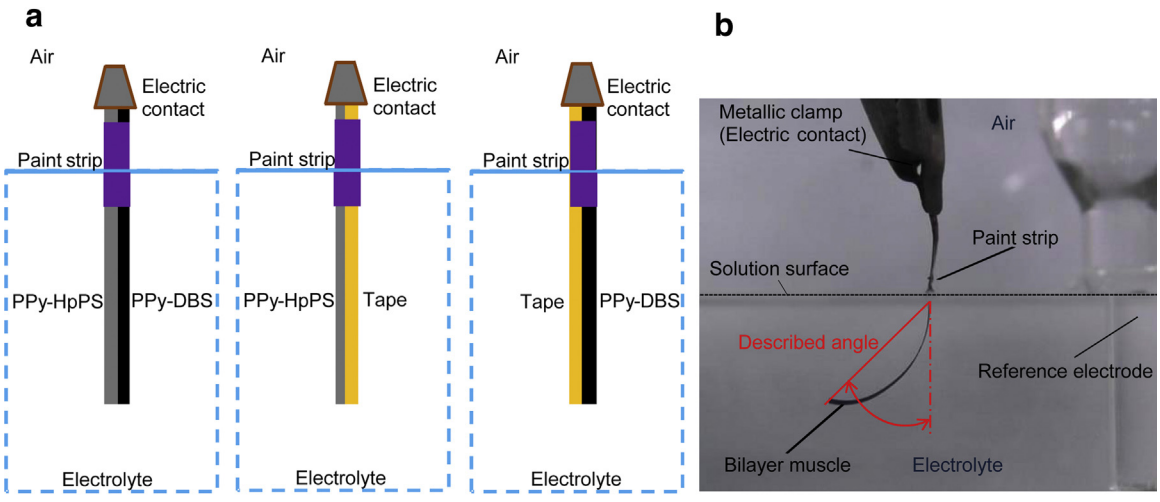

Fig. 1. (a) Scheme of the PPy-HpPS/PPy-DBS, PPy-HpPS/tape and PPy-DBS/tape bilayer artificial muscles with the relative position of the two constitutive layers as in the checked muscles, transversal paint strip and alligator metal electric contact. (b) A picture of a bilayer muscle in the cell and determination of the described angle.

3. Results and discussion

3.1. Electrogeneration of the (PPY-HpPS/PPy-DBS) Bilayer Muscle

The AISI316 stainless steel working electrode was first coated with a polypyrrole-dodecylbenzenesulfonic acid (PPy-DBS) film following the procedure above described by consumption of 5.76C. Fig. 2a shows the evolution of the electrode potential. The coated electrode was then rinsed and kept in ultrapure water for 1 day in order to eliminate the adsorbed organic acid molecules. The coated electrode was then dried in air at room temperature during one day.

After that the Pt/PPy-DBS electrode was used as the working electrode (WE) in 50 mL of 0.05 M HpPS and 0.20 M pyrrole aqueous solution. A PPy-HpPS film was electrogenerated following the above-described procedure by consumption of 3.06C. Fig. 2b shows the evolution of the electrode potential. Once generated the steel plate coated with the PPy-HpPS/PPy-DBS bilayer was rinsed with water and dried in air at room temperature for 1 day. Then the borders of the steel coated electrode were scrapped and the two PPy-HpPS/PPy-DBS bilayer films (one by steel side) were peeled off from the metal. Those films were cut into smaller longitudinal strips each 15 × 1 mm, and 40 μm thick. The mass of every film was determined using a microbalance. Each film was painted with a transversal paint strip on both film sides from 2.0 mm to 5.0 mm of the upper border. The paint closes the pores, avoids the electrolyte capillarity towards the metal clamp required for the electrical contact and the concomitant electrolyte discharge on the metal clamp during experiments.

3.2. Bending artificial muscles

The three bilayer muscles, PPy-HpPS/PPy-DBS, PPy-HpPS/tape and tape/PPy-DBS, were checked in parallel in the same electrolyte and under the same electrochemical conditions.

Fig. 1a presents a scheme of each of the three studied bilayers showing the relative position (left side/right side) of every layer kept during the experiments, the transversal paint strip and the clamp for the electrical contact. This relative position of the two layers is a key point to get the reaction-driven ionic exchanges from the angular movements (Section 3.5). Fig. 1b presents a picture of a bilayer muscle in the experimental cell and how the described angle, or angular displacement is obtained. The angular displacement is video recorded in parallel to the electrochemical experiments.

3.3. Stationary Voltammetric (i/E) and Coulovoltammetric (Q/E) Responses

Each of those bilayer muscles was submitted to 40 consecutive voltammetric cycles between −0.4 V and 0.7 V at a scan rate of 10 mV s^{-1} at room temperature in 0.5 M NaCl aqueous solution. The consecutive voltammograms show increasing currents. After 40 cycles stationary voltammetric responses are got: the consecutive voltammograms overlap. Any previous structural memory [40–43] from the electrogenerated polypyrrole films was thus erased. Once the stationary response was attained the potential limits can be changed getting stationary responses after only two consecutive potential cycles.

Fig. 3a, b and c show the stationary voltammetric responses obtained from PPy-HpPS/PPy-DBS, PPy-HpPS/tape and tape/PPy-DBS, respectively, bilayer muscles between −1.0 V and 0.7 V at 10 mV s^{-1} in 0.5 M NaCl aqueous solution.

Fig. 3d, e and f shows the coulovoltammetric (Q/E) response from a PPy-HpPS/PPy-DBS, PPy-HpPS/tape and tape/PPy-DBS bilayer muscles got by integration of the voltammetric response from Fig. 3a, b and c, respectively. Practically closed Q/E loops were attained: anodic charges equal cathodic charges indicating that only reversible film oxidation/reduction reactions are there involved [44]. Any variation of the Q/E slope indicates a parallel change on the reaction rate (r) [44–46]. The charge (Q) controls the number (n) of exchanged ions:

$$dn = \frac{dQ}{zF} \tag{1}$$

where z is the valence of the ion and F is the Faraday constant. For an empirical potential sweep rate ν=(dE/dt) the PPy reaction rate results:

$$r = \frac{dn}{dt} = \frac{{}^{d}Q/_{z}F}{{}^{d}E/_{\nu}} = \frac{dQ\ \nu}{dE\,zF} \tag{2}$$

where dQ/dE is the slope at any point on Figs. 3d, e and f [44]. Points 2, 4 and 5 correspond to inflexion points (slope changes) that mean changes on the reaction rates. The maximum 1 and the

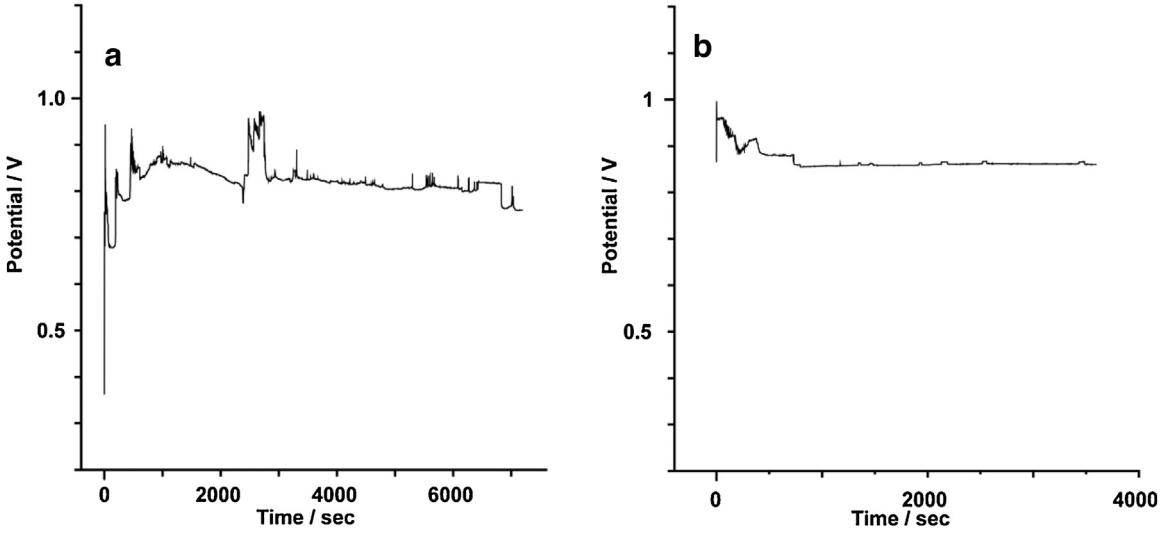

Fig. 2. Evolution of the potential during the electropolymerization (a) of PPy-DBS by applying a constant anodic current density of 0.5 mA cm^{-2} for 7200 seconds through the stainless steel working electrode in 0.25 M DBSA and 0.15 M pyrrole aqueous solution at 0 °C and (b) of PPy-HpPS by applying a constant anodic current density of 0.5 mA cm^{-2} for 3600 seconds through the PPy-DBS coated stainless steel working electrode in 0.05 M HpPS and 0.20 M pyrrole aqueous solution at 0 °C.

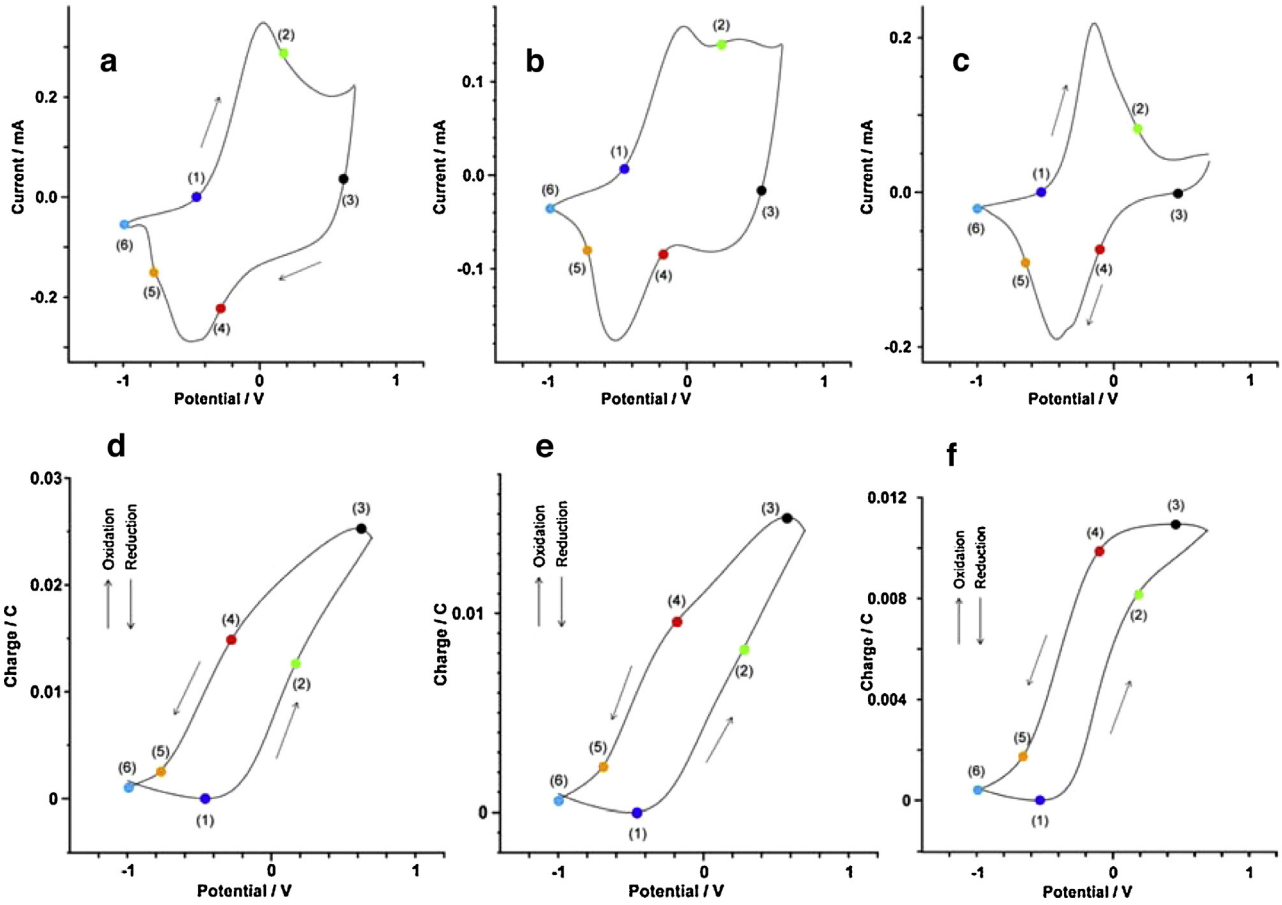

Fig. 3. Stationary voltamnograms using a self-supported (a) PPy-HpPS/PPy-DBS film, (b) PPy-HpPS film and (c) PPy-DBS film from −1.0 V to 0.7 V, at 10 mV s^{-1} in 0.5 M NaCl aqueous solution at room temperature. Coulovoltammetric responses obtained by integration of the voltammograms (d) from Fig. 3a, (e) from Fig. 3b and (f) from Fig. 3c.

minimum 3 correspond to changes from the film reductions (negative charge increments) to the film oxidations (positive charge increments) and from film oxidations (positive charge increments) to the film reductions (negative charge increments), respectively. Point 6 indicates the cathodic potential limit.

The charge involved in the PPy-HpPS/PPy-DBS cycle (Fig. 3d) is close to the sum of those charges involved in the tape/PPy-DBS and PPy-HpPS/tape cycles (Fig. 3e and f). After clarification of the reaction driven ionic exchanges between the two polypyrrole blends and the electrolyte (Section 3.5) the structural changes driven by the reactions for the different potential ranges related to different reaction rates will be identified in Section 3.6.

3.4. Influence of the Cathodic Potential Limit

Fig. 4a, b and c show stationary Q/E responses from the PPy-HpPS/PPy-DBS, PPy-HpPS/tape and tape/PPy-DBS bilayer muscles, respectively, after consecutive potential sweeps from a different cathodic potential limit every time, ranging from −0.6 V to −2.0 V (each loop minimum was taken as the charge zero origin)

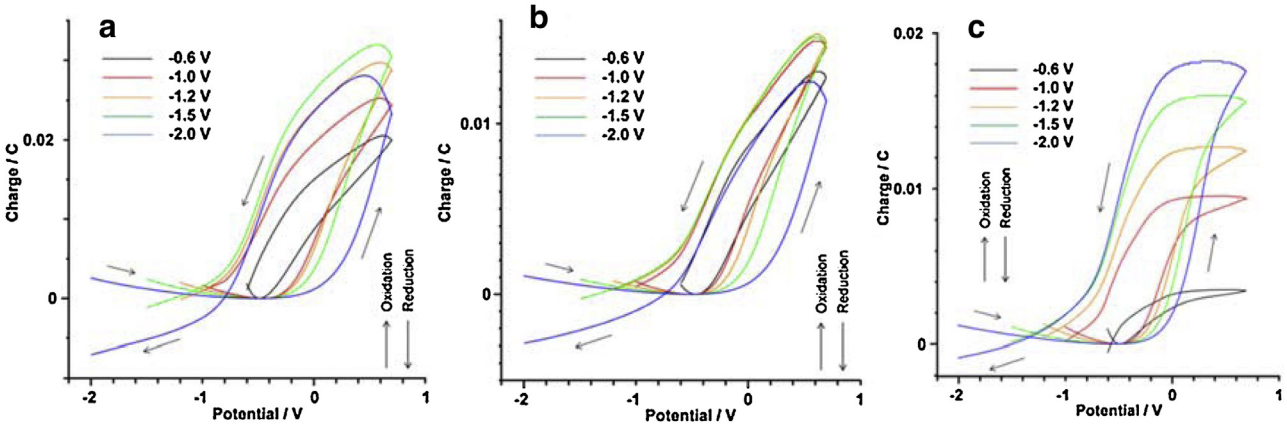

Fig. 4. Coulovoltammetric responses in NaCl aqueous solutions from a different cathodic potential limit (ranging from −0.6 V to −2.0 V) up to the same anodic potential limit of 0.7 V every time using (a) the PPy-HpPS/PPy-DBS bilayer muscle (b) PPy-HpPS/tape bilayer muscle and (c) tape/PPy-DBS bilayer muscle.

up to the same anodic potential limit of 0.7 V every time. Coulovoltammetric responses from cathodic potential limits lower than −1.0 V show a closed loop: the film oxidation charge equals the film reduction charge [44].

For more cathodic potential limits every coulovoltammogram shows two different parts. The closed loop on the right side quantifies the charge (maximum to minimum range) consumed by the reversible film oxidation/reduction in the full studied potential range. For PPy-DBS (Fig. 4c) the redox charge of the closed loop increases with the cathodic potential limit. The PPy-HpPS redox charge increases with the cathodic potential limit until −1.5 V and then decreases (Fig. 4b) for higher cathodic potential limits.

The open part on the left side defines a negative charge increment (irreversible reduction charge) from the initial potential to the final potential of the cycle. When the polypyrrole film was generated in presence of small stable anions this irreversible charge only starts at more cathodic potential limits than −3 V [46]. Thus, irreversible charges in Fig. 4 are attributed to the irreversible evolution of hydrogen from the HDBS or from the HpPs components of the polypyrrole blends [44,46]. On consecutive cycles each consecutive coulovoltammetric response presents a negative shift of the charge (charge creeping) [33] equal to this irreversible charge.

3.5. Dynamo-voltammetric (angle/E) responses: reaction-driven ionic exchanges

Each video-frame from the video recorded in parallel to the potential sweeps gives the angular position of the muscle at the concomitant potential as indicated in Fig. 1b. Fig. 5a, b and c show the angular displacements (evolution of the angular position) of the three studied bilayer muscles at each potential during the potential cycle. Those are dynamo-voltammetric muscular responses: evolution of the angular position with the potential. Potentials at points (1), (1′), (2), (3), (4) and (5) correlate those on voltammetric (Fig. 3a–c) and coulovoltammetric (Fig. 3d–f) responses. Pictures and schemas from Fig. 6a–c show the angular position and the angular displacements (arrows), respectively, of the three studied bilayer muscles between those points.

The angular displacement of the asymmetric bilayer is the result of ionic exchanges in each of the two PPy blend films. Those ionic exchanges can be clarified by electrochemo-dynamical characterization of each pPy blend/tape bilayer muscle, keeping the PPy blend film the same relative position that it has in the asymmetric bilayer [37].

3.5.1. Dynamo-voltammetric responses from PPy-HpPS/tape bilayer muscles

The PPy-HpPS/tape muscle shows (Figs. 5 b and 6 b) a bending displacement of 14 degrees during the potential cycle and a clockwise creeping dynamical effect (the initial position is not recovered at the end of the cycle) of 1.5 degrees per cycle. Going closer the dynamo-voltammetric response (Fig. 5b) shows a clockwise bending movement of the bilayer from point (1) to point (2) indicating that the PPy-HpPS shrinks by oxidation. According with the basic electrochemical reactions from the different families of conducting polymers the oxidation in this electrolyte is initiated by expulsion of Na^+ driven by the reaction:

$$\left[(PPy^0)(pPS^-)_n(Na^+)_n(H_2O)_m\right]_{gel} \rightleftarrows (PPy^{n+})(pPS^-)_n + n(Na^+) + m(H_2O) + n(e^-)_{metal} \quad (3)$$

where PPy° represents the active sites on the polypyrrole chains that will store positive charges after oxidation becoming PPy^{n+}, n being the number of removed electrons (e^-) per chain and the water molecules are exchanged to keep the osmotic pressure balance forming a dense gel (indicated by subindex gel). The dense gel shrinks during oxidation from point 1 to point 2 by expelling balancing cations and solvent and swells during reduction from point 4 to point 6 to lodge cations and solvent.

From point (2) until point (3) the anticlockwise bending movement of the bilayer indicates that the PPy-HpPS swells during oxidation by incorporation of anions. The driving reactions being:

$$(PPy^0HpPS) + n(Cl^-) + m(H_2O) \rightleftarrows \left[(PPy^{n+}HpPS)(Cl^-)_n(H_2O)_m\right]_{gel} + n(e^-)_{metal} \quad (4)$$

where Cl^- are the anions exchanged to keep the film electroneutrality. Reaction 4 should indicate that the HpPS acid remaining inside the PPy film does not dissociates in this potential range for a partially oxidized polypyrrole [37,39]. The gel swells by oxidation (lodging anions and solvent) and shrinks by reduction (expelling them). The HpPS remains trapped forcing the exchange of anions from the electrolyte during oxidation reduction [37]. From point (3), to point (4) the clockwise bending movement indicates that the polymer reduces and shrinks by expulsion of Cl^- (reaction 4 backwards).

As a partial conclusion the PPy-HpPS film shrinks/swells during oxidation/reduction, respectively, in NaCl aqueous solution by exchange of cations driven by reaction 3 at the more cathodic potential range of the cycle. The film swells/shrinks by oxidation/reduction, respectively, exchanging anions driven by reaction 4 at the more anodic potential range of every cycle. The result of two

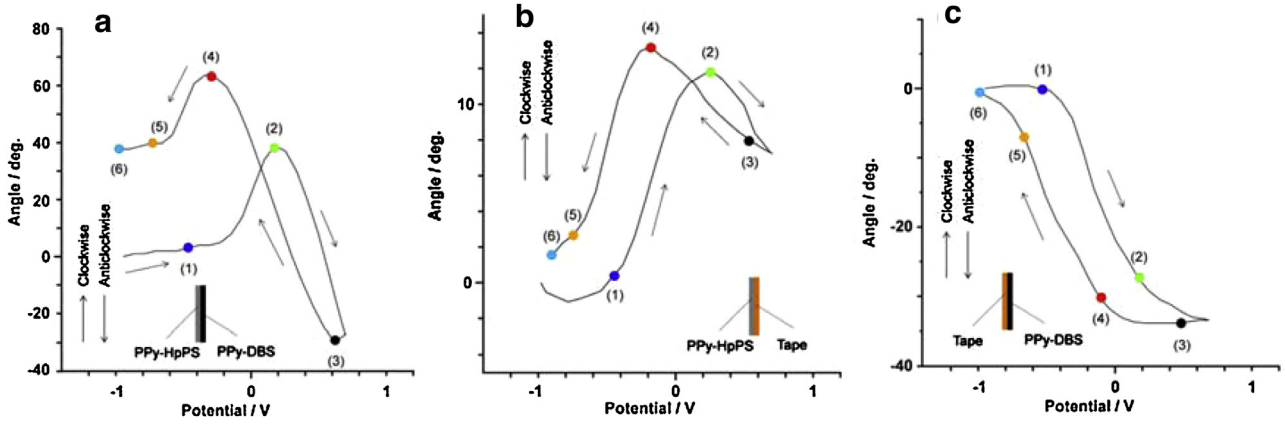

Fig. 5. Dynamo-voltammetric responses: evolution of the described angle as a function of the applied potential during a potential cycle from the different bilayers artificial muscles: (a) PPy-HpPS/PPy-DBS, (b) PPy-HpPS/tape and (c) PPy-DBS/tape artificial muscles, during potential sweep at 10 mV s^{-1} in 0.5 M NaCl aqueous solution.

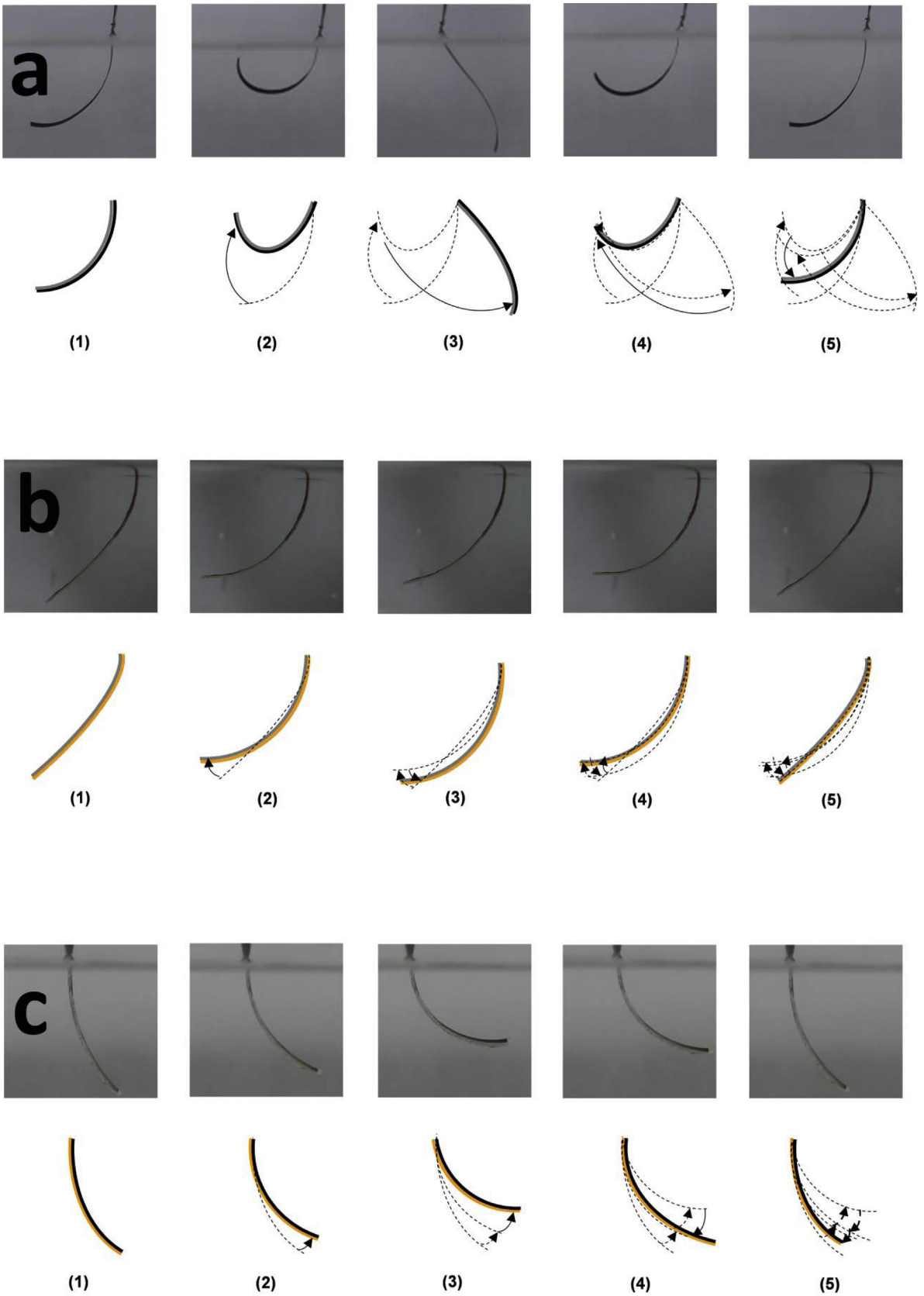

Fig. 6. Pictures and schemes of the different bilayers artificial muscles: (a) PPy-HpPS/PPy-DBS, (b) PPy-HpPS/tape and (c) PPy-DBS/tape artificial muscles, in 0.5 M NaCl aqueous solution during voltammetric experiments between −1.0 and 0.7 V at 10 mV s^{-1} at room temperature. The points (1), (2), (3), (4) and (5) correlate with both, the coulovoltammograms shown in Fig. 3 and the evolution of the described angles shown in Fig. 5.

consecutive ionic exchanges during the potential cycle is two go and back bending movements (Fig. 5b and schemas from 6 b) per cycle.

3.5.2. Dynamo-voltammetric responses from tape/PPy-DBS bilayer muscles

Responses from the tape/PPy-DBS muscle (Figs. 3 c, 5 c and 6 c) show anticlockwise bending movement during oxidation. That means that the PPy-DBS film shrinks by expulsion of cations. During reduction the clockwise bending movement of the bilayer indicates that the conducting polymer swells due to the entrance of cations from the solution. The oxidation/reduction is driven by the reaction [38]:

$$\left[(PPy^0)(DBS^-)_n(Na^+)_n(H_2O)_m\right]_{gel} \rightleftarrows (PPy^{n+})(DBS^-)_n + n(Na^+) + m(H_2O) + n(e^-)_{metal} \quad (5)$$

The described bending amplitude per cycle was 35 degrees.

The dense gel shrinks during oxidation by expelling cations and solvent and swells during reduction to lodge cations and solvent (Fig. 5c).

3.5.3. Dynamo-voltammetric responses from PPy-HpPS/PPy-DBS bilayer muscles

Using those ionic exchanges inside the concomitant potential ranges for each conducting polymer/tape bilayer, angular movements form the PPy-HpPS/PPy-DBS asymmetric bilayer muscle (Fig. 5a) can now be clarified. A reduction charge flows through the PPy-HpPS/PPy-DBS muscle under potential sweep from −1.0 V up to the coulovoltammetric minimum (Fig. 3d), point (1). This charge is not efficient to bend the muscle (Fig. 5a): that means that most of the charge is consumed by irreversible hydrogen evolution from the two films. From (1) to (2) a fast oxidation occurs (high slope from Fig. 3d) promoting a clockwise bending movement (Fig. 6a, pictures and schema 1–2). From point 1 to point 2 both constituent layers oxidize (Fig. 3e and f) and shrink by expelling Na^+ (reactions 3 and 5 forwards). The final results should be an antagonist dynamic effect with both films contracting giving a shorter bilayer. Nevertheless, the PPy-HpPS shrinks faster originating the observed clockwise bending movement of 40 degrees. This is a surprising positive result taking into account that the full amplitude described by the PPy-HpPS/tape muscle was only 14 degrees (Section 3.5.1). Here, in presence of antagonist effects, the asymmetric bilayer describes larger amplitude.

From (2) to (3) a slower oxidation rate (lower slope in Fig. 3b) gives a large anticlockwise displacement (Figs. 5 a and 6 a from 2 to 3). In this potential range the PPy-HpPS film swells by oxidation, following reaction 4 forwards with entrance of Cl^- (Fig. 5c) and pushes the bending bilayer. In parallel the PPy-DBS film shrinks by oxidation (Figs. 5 c and 6 c) with expulsion of Na^+, reaction 5 forwards, pulling the bilayer. The two layers cooperate (dynamic cooperation) to get an anticlockwise amplitude of 69 degrees. This amplitude is over five times the amplitude described by cycling the PPy-HpPS/tape muscles (14 degrees) and almost two times the angle described by the tape/PPy-DBS muscle (35 degrees) in the full potential range.

From (3) to (4) a slow reduction occurs (Fig. 3d) while the muscle bends clockwise (Figs. 5 a and 6 a 3–4). At the coulovoltammetric maximum, point (3) Fig. 3d, both polymers present their most oxidized state. During reduction up to point (4) the PPy-HpPS film, as stated above, shrinks by expulsion of Cl^- pulling the muscle and the PPy-DBS film swells by entrance of Na^+ pushing the muscle. Thus, volume variations originated by both film reactions cooperate (cooperative dynamic effect) in that potential range to bend the asymmetric bilayer (Fig. 6a, from 3 to 4). The bending amplitude was (Fig. 6a) 93 degrees. This is over fifteen times the amplitude got by the PPy-HpPS/tape muscles (6 degrees in the same potential range) and almost three times the amplitude described by the tape/PPy-DBS muscle in the full potential range (35 degrees).

Finally from (4) to (5) the film reduces (Fig. 3d) very fast and then slowly from (5) to (6), while bending anticlockwise (Figs. 5 a and 6 a 4–5). Both constituent films, the PPy-HpPS and the PPy-HpPS, swell by entrance of Na^+ originating an antagonist dynamic effect. The PPy-HpPS swelling results most efficient pushing the film 15 degrees anticlockwise (Fig. 6a).

The bending movement of the asymmetric bilayer is not fully reversible under cycling presenting a clockwise creeping effect (different between the muscle position at the beginning and at the end of the cycle). Creeping effects were attributed to the irreversible charge consumed at those potentials [33]. Antagonist dynamic effects taking place here at those cathodic potentials enhance the creeping effect. The creeping effect was clockwise 38 degrees: the response to consecutive voltammograms are always angular displacements of 93 degrees but each dynamo-voltammetric response sifts 38 degrees clockwise related to the previous one (chemical creeping effect).

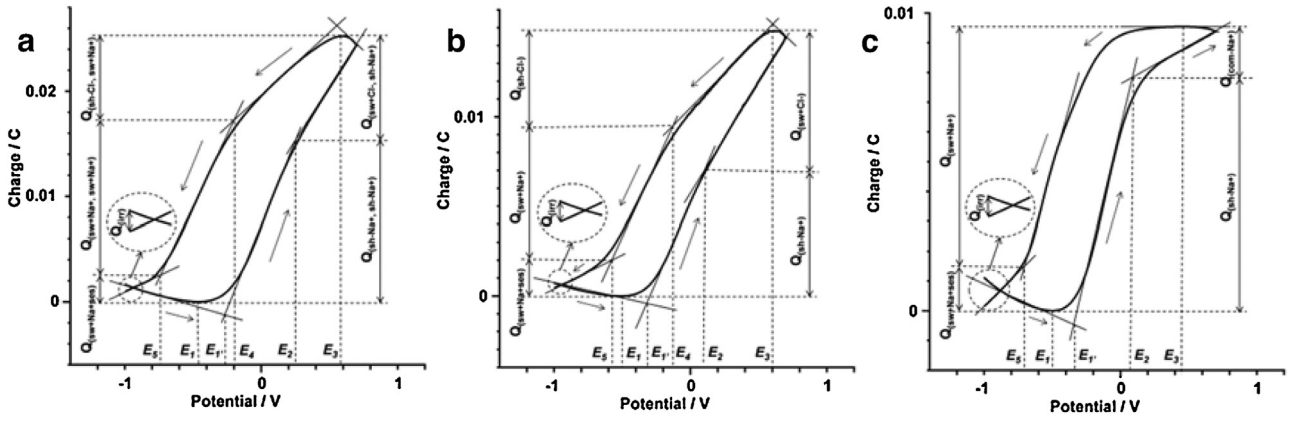

Fig. 7. Coulovoltammetric response from (a) PPy-HpPS/PPy-DBS, (b) PPy-HpPS/tape and (c) PPy-DBS/tape muscles when the potential was swept between −1.0 V, and 0.7 V at 10 mV s^{-1} in 0.5 M NaCl aqueous solution, showing abrupt slope variations related to abrupt changes of the reaction rates (dQ/dt = dn/dt, were n = Q/F is the number of exchanged electrons and ions and F the Faraday constant) due to reaction change or structural transitions inside the film driven by the reactions. Each of the abrupt slope changes indicates a potential characteristic of a structural/reaction change: E_1, E_1', E_2, E_3, E_4, E_5; the charge difference between two characteristic potentials corresponds to the charge of the concomitant structural process.

3.6. Reaction-driven structural changes

In Section 3.3 it was stated that coulovoltammetric slope variations quantify, through Eq. (2), changes of the reaction rates. Thus, Fig. 3d–f, are presented again, Fig. 7a, b and c, identifying now the different slope changes during a potential cycle. Once identified the reactions (reactions 1 and 2) driven the muscular action the different reaction-driven structural processes linked to each change of the reaction rate can be analyzed according with previous results [37,46,47]. Starting and finishing in an oxidized swollen film exchanging anions four reaction-driven structural processes were identified from the closed Q/E loop: reduction-shrinking, reduction-compaction, oxidation-relaxation and oxidation-swelling [44]. Cation-driven reactions, PPy-DBS here, present (Figs. 5 c and 7 c) six reaction-driven structural changes in one loop: reduction-relaxation, reduction-swelling, reduction vacuolar formation, oxidation-vacuolar relaxation, oxidation shrinking and oxidation-compaction [46]. For the PPy-HpPS the ionic (Fig. 5b) and structural (Fig. 7b) changes must be related to the consecutive exchange of cations and anions: oxidation-shrinking with expulsion of Na^+ from E_1' to E_2; oxidation-swelling with entrance of Cl^- from E_2 to E_3, reduction-shrinking with expulsion of Cl^- from E_3 to E_4, reduction-swelling with entrance of Na^+ from E_4 to E_5, reduction-lamellar formation going on the Na^+ entrance from E_5 through E_6 until E_1 and oxidation with vacuolar relaxation around E_1'. Reaction-driven structural changes in the asymmetric bilayer (Fig. 7a) are a result of the simultaneous structural changes in both constituent films.

3.7. Coulo-dynamic (Q/angle) responses

Bilayer muscles based on CPs are claimed as Faradaic polymeric motors: described angles follow a linear dependence of the consumed charge [48–50]. This linearity is kept by both, CPs exchanging cations or anions during its oxidation/reduction [38,50]. The complex ionic exchanges here identified require checking if the actuator still behaves as a Faradaic motor.

By combination of Figs. 3 and 5 the coulo-dynamic (charge-angle) responses from the three-studied bilayer muscles, Fig. 8, were attained. The coulo-dynamic behavior of the PPy-HpPS/PPy-DBS muscle (Fig. 8a) is similar to that of the PPy-HpPS/tape muscle (Fig. 8b) illustrating the preponderant electro-chemo-mechanical contribution of the PPy-HpPS to the bending dynamics of the asymmetric bilayer muscle. Both responses show two, in average, linear oxidation/reduction sections each related to the prevalent reversible exchange of anions or cations above described for the PPy-HpPS layer: 1–2 (oxidation with Na^+ expulsion) and 4–6 (reduction with Na^+ entrance) and point 2–3 (oxidation with Cl^- entrance) and 3–4 (reduction with Cl^- expulsion). Deviation from the linearity and dynamic hysteresis between the anodic and cathodic displacement for the same angle have been attributed to a dynamic hysteresis on the entrance/exit of water molecules by osmosis, a physical effect that always follow the faradaic exchange of ions [34,51–53]. The coulo-dynamic behaviour of the tape/PPy-DBS bilayer muscle in NaCl aqueous solution shows, Fig. 7c, a linear dependence of the bending angle with the consumed charge, corroborating the faradaic origin of the movement driven by reaction 1: the number of electrons extracted from or injected to the polymer chains controls either the number of exchanged cations (Eq. (3)), the film volume variation, the stress gradient at the layer/layer interface and the bending angle. The PPy-DBS film shrinks by oxidation due to the expulsion of Na^+ towards the solution and swells by reduction due to the entrance of Na^+. The flattened 8 shape with some dynamic hysteresis (different angle for the same charge) between the anodic and the cathodic branches has been attributed to osmotic (hysteresis) and electro-osmotic (double loop formation) exchange of water following the ionic concentration variation [39].

Creeping effects (angular displacement from the beginning to the end point of each potential cycle Fig. 7b and c) has been related to some irreversible hydrogen evolution overlapping ionic exchanges at the most cathodic potentials [33].

Form the comparative characterization of the three bilayers we can summarize that the oxidation of the PPy-HpPS/PPy-DBS asymmetric bilayer muscle is a result of the ionic exchanges driven by the electrochemical reactions in the two studied polypyrrole blends.

Fig. 7a shows a large chemical creeping effect (difference between the muscle position at the beginning and at the end of the potential cycle) of the asymmetric bilayer when compared with the low creeping effect of those bilayers including a tape (Fig. 7b and c). The presence of antagonistic dynamic effects in the asymmetric bilayer muscle amplifies the creeping effect related to those presented by each of the polypyrrole/tape bilayer muscles.

The bending asymmetric bilayer gives, as expected, cooperative (synergic) dynamic effects when the electrochemical reaction promotes reverse ionic exchanges and reverse volume variations (swelling/shrinking or shrinking/swelling) in the two constituent films. This cooperation results in a high actuation efficiency: the angle described per unit of consumed charge (slopes from the Q/D

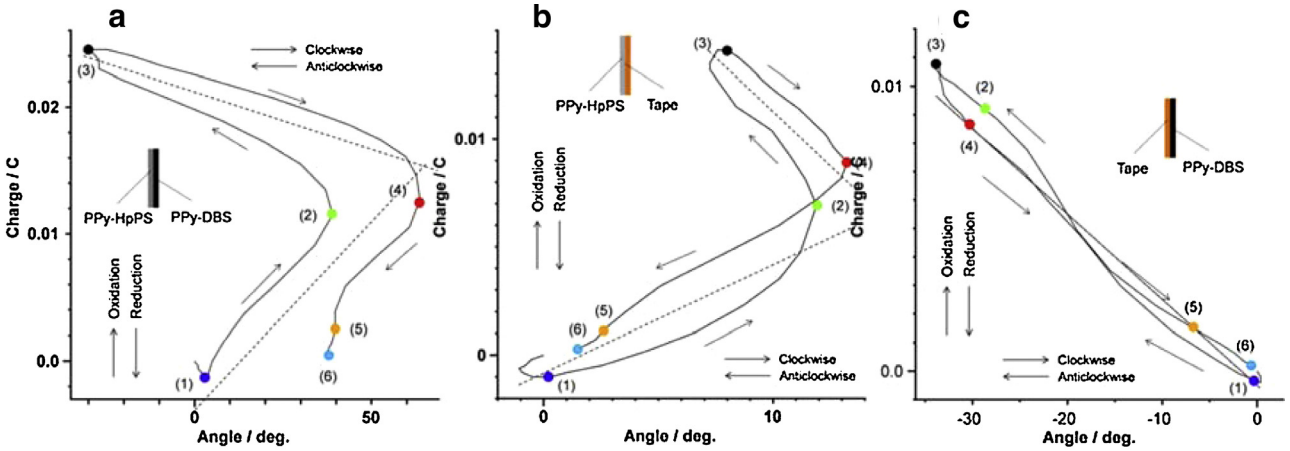

Fig. 8. Coulo-dynamic responses (bending angle described by the muscles *versus* consumed charges) during voltammetric experiments between −1.0 and 0.7 V at 10 mV s^{-1} from the three studied artificial bilayer muscle, (a) PPy-HpPS/PPy-DBS, (b) PPy-HpPS/tape and (c) PPy-DBS/tape, in NaCl aqueous solution.

response) is higher (up to 15 fold) those described under parallel electrochemical control by each of the two CP/tape bilayer muscles.

When the bilayer reaction (oxidation or reduction) drives volume variations of the two films in the same direction (swelling/swelling or shrinking/shrinking) due to parallel entrance or expulsion of ions in both layers originate antagonist forces at the interface: the bending direction and the bending amplitude is dominated by the most efficient layer, the CP layer having the most efficient volume variation per unit of charge, the PPy-HpPS here. The presence of antagonist effect amplifies creeping effects of the constitutive layers that could be used as a tool for the quantification of the relative. Antagonist dynamic effects complicate the control of the muscle movement for robotic applications.

Asymmetric bilayer muscles while working under cooperative effects are linear faradaic muscle: the large described angle is a linear function of the consumed charge getting an excellent control of the muscle movement and position.

4. Conclusions

Here we have presented a comparative study of the coulo-voltammetric (Q/E), dynamo-voltammetric (angle/E) and coulo-dynamic (Q/angle) behavior of the (PPy-HpPS/PPy-DBS) asymmetric bilayer muscle and the two PPy-HpPS/tape and tape/PPy-DBS bilayer muscles in NaCl aqueous solution.

The electrochemical reactions of the PPy-HpPS film and their induced ionic exchanges control the bending behavior of the asymmetric bilayer muscle.

When the ionic exchanges driven by the reaction (oxidation or reduction) are opposed in each of the constituent layers (anion entrance/cation exit, or cation entrance/anion exit) the asymmetric bilayer originates cooperative dynamic actuation of the constituent layers (swelling/shrinking, or shrinking/swelling) and the amplitude of the described angular movement is greater (synergic dynamical effect) than any of those described by the PPy-HpPS/tape or the tape/PPy-DBS bilayer muscles in the same electrolyte.

When the reaction-driven exchange of ions gives parallel volume variations in the two constitutive layers (swelling/swelling or shrinking/shrinking) originates antagonist dynamic actuation of the two layers. The layer having the most efficient volume change per unit of charge controls the bending movement of the asymmetric bilayer: PPy-HpPS here. The antagonist actuation originates narrower angles described per unit of consumed charge (Q/angle slope) and improves creeping effects.

For the development of efficient asymmetric bilayer muscles it must be avoided the presence of antagonist effect and that of irreversible reactions consuming charge without generation of film volume changes, as hydrogen evolution from the acid organic components at high cathodic potentials or proton's expelling at high anodic potentials.

Acknowledgments

The authors acknowledge the financial support from the Kyushu Institute of Technology, the Spanish Government (MCINN) Projects MAT2011-24973 and the Seneca Foundation project 19253/PI/14. J.G. Martinez acknowledges Spanish Education Ministry for a FPU grant (AP2010-3460).

References

[1] T.F. Otero, Conducting Polymers, Electrochemistry, and Biomimicking Processes, in: R.E. White, J.O. Bockris, B.E. Conway (Eds.), Mod. Asp. Electrochem., Springer, US, New York, 1999, pp. 307–434. (accessed 09.01.13) http://link.springer.com/chapter/10.1007/0-306-46917-0_3.
[2] T.F. Otero, Conducting Polymers: Bioinspired Intelligent Materials and Devices, RSC, 2015.
[3] T.F. Otero, Biomimetic Conducting Polymers: Synthesis, Materials, Properties, Functions, and Devices, Polym. Rev. 53 (2013) 311–351, doi:http://dx.doi.org/10.1080/15583724.2013.805772.
[4] T.F. Otero, J.G. Martinez, Biomimetic intracellular matrix (ICM) materials, properties and functions Full integration of actuators and sensors, J. Mater. Chem. B. 1 (2013) 26–38, doi:http://dx.doi.org/10.1039/C2TB00176D.
[5] P. Atkins, J. De Paula, Physical Chemistry, 7th ed., OUP Oxford, Oxford, 2002.
[6] L. Stryer, Biochemistry, W.H Freeman and Company, New York, 1995.
[7] T.F. Otero, J.G. Martinez, J. Arias-Pardilla, Biomimetic electrochemistry from conducting polymers. A review Artificial muscles, smart membranes, smart drug delivery and computer/neuron interfaces, Electrochimica Acta. 84 (2012) 112–128, doi:http://dx.doi.org/10.1016/j.electacta.2012.03.097.
[8] L. Bay, K. West, P. Sommer-Larsen, S. Skaarup, M. Benslimane, A Conducting Polymer Artificial Muscle with 12% Linear Strain, Adv. Mater. 15 (2003) 310–313, doi:http://dx.doi.org/10.1002/adma.200390075.
[9] M.S. Cho, J.J. Choi, T.S. Kim, Y. Lee, In situ three-dimensional analysis of the linear actuation of polypyrrole micro-rod actuators using optical microscopy, Sens. Actuators B-Chem. 156 (2011) 218–221, doi:http://dx.doi.org/10.1016/j.snb.2011.04.021.
[10] S.Y. Chu, H. Peng, P.A. Kilmartin, G.A. Bowmaker, R.P. Cooney, J. Travas-Sejdic, Effect of deposition current density on the linear actuation behaviour of PPy (CF3SO3) films, Curr. Appl. Phys. 8 (2008) 324–327, doi:http://dx.doi.org/10.1016/j.cap.2007.10.024.
[11] A. DellaSanta, D. DeRossi, A. Mazzoldi, Characterization and modelling of a conducting polymer muscle-like linear actuator, Smart Mater. Struct. 6 (1997) 23–34.
[12] B.K. Gu, Y.A. Ismail, G.A. Spinks, S.I. Kim, I. So, S.J. Kim, A Linear Actuation of Polymeric Nanofibrous Bundle for Artificial Muscles, Chem. Mater. 21 (2009) 511–515, doi:http://dx.doi.org/10.1021/cm802377d.
[13] R. Kiefer, S.Y. Chu, P.A. Kilmartin, G.A. Bowmaker, R.P. Cooney, J. Travas-Sejdic, Mixed-ion linear actuation behaviour of polypyrrole, Electrochimica Acta. 52 (2007) 2386–2391, doi:http://dx.doi.org/10.1016/j.electacta.2006.08.058.
[14] F. Vidal, C. Plesse, G. Palaprat, A. Kheddar, J. Citerin, D. Teyssie, et al., Conducting IPN actuators: From polymer chemistry to actuator with linear actuation, Synth. Met. 156 (2006) 1299–1304, doi:http://dx.doi.org/10.1016/j.synthmet.2006.09.012.
[15] K. Yamato, K. Kaneto, Tubular linear actuators using conducting polymer, polypyrrole, Anal. Chim. Acta. 568 (2006) 133–137, doi:http://dx.doi.org/10.1016/j.aca.2005.12.030.
[16] A. DellaSanta, D. DeRossi, A. Mazzoldi, Performance and work capacity of a polypyrrole conducting polymer linear actuator, Synth. Met. 90 (1997) 93–100.
[17] T.F. Otero, E. Angulo, J. Rodríguez, C. Santamaría, Electrochemomechanical properties from a bilayer: polypyrrole/non-conducting and flexible material—artificial muscle, J. Electroanal. Chem. 341 (1992) 369–375, doi:http://dx.doi.org/10.1016/0022-0728(92) 80495-P.
[18] Q. Pei, O. Inganas, Conjugated Polymers and the Bending Cantilever Method—Electrical Muscles and Smart Devices, Adv. Mater. 4 (1992) 277–278, doi:http://dx.doi.org/10.1002/adma.19920040406.
[19] G. Alici, N.N. Huynh, Predicting force output of trilayer polymer actuators, Sens. Actuators —Phys. 132 (2006) 616–625, doi:http://dx.doi.org/10.1016/j.sna.2006.02.046.
[20] T.F. Otero, J.G. Martinez, J. Arias-Pardilla, Biomimetic electrochemistry from conducting polymers. A review: Artificial muscles, smart membranes, smart drug delivery and computer/neuron interfaces, Electrochimica Acta. 84 (2012) 112–128, doi:http://dx.doi.org/10.1016/j.electacta.2012.03.097.
[21] Q. Pei, O. Inganas, Electrochemical Applications of the Bending Beam Method .1. Mass-Transport and Volume Changes in Polypyrrole During Redox, J. Phys. Chem. 96 (1992) 10507–10514, doi:http://dx.doi.org/10.1021/j100204a071.
[22] Q. Pei, O. Inganas, Electrochemical Applications of the Bending Beam Method .2. Electroshrinking and Slow Relaxation in Polypyrrole, J. Phys. Chem. 97 (1993) 6034–6041, doi:http://dx.doi.org/10.1021/j100124a041.
[23] G.Y. Han, G.Q. Shi, Conducting polymer electrochemical actuator made of high-strength three-layered composite films of polythiophene and polypyrrole, Sens. Actuators B-Chem. 99 (2004) 525–531, doi:http://dx.doi.org/10.1016/j.snb.2004.01.001.
[24] G.Y. Han, G.Q. Shi, High-response tri-layer electrochemical actuators based on conducting polymer films, J. Electroanal. Chem. 569 (2004) 169–174, doi:http://dx.doi.org/10.1016/j.jelechem.2004.02.025.
[25] E. Ochoteco, J.A. Pomposo, M. Bengoechea, H. Grande, J. Rodriguez, Assembled cation-exchange/anion-exchange polypyrrole layers as new simplified artificial muscles, Polym. Adv. Technol. 18 (2007) 64–66, doi:http://dx.doi.org/10.1002/pat.796.
[26] U.L. Zainudeen, M.A. Careem, S. Skaarup, PEDOT and PPy conducting polymer bilayer and trilayer actuators, Sens. Actuators B-Chem. 134 (2008) 467–470, doi:http://dx.doi.org/10.1016/j.snb.2008.05.027.
[27] J. Liu, Z. Wang, X. Xie, H. Cheng, Y. Zhao, L. Qu, A rationally-designed synergetic polypyrrole/graphene bilayer actuator, J. Mater. Chem. 22 (2012) 4015–4020, doi:http://dx.doi.org/10.1039/c2jm15266e.
[28] M. Fuchiwaki, K. Tanaka, K. Kaneto, Planate conducting polymer actuator based on polypyrrole and its application, Sens. Actuators-Phys. 150 (2009) 272–276, doi:http://dx.doi.org/10.1016/j.sna.2009.01.011.

[29] Y. Naka, M. Fuchiwaki, K. Tanaka, A micropump driven by a polypyrrole-based conducting polymer soft actuator, Polym. Int. 59 (2010) 352–356, doi:http://dx.doi.org/10.1002/pi.2762.
[30] T.F. Otero, J.G. Martinez, Artificial Muscles: A Tool To Quantify Exchanged Solvent during Biomimetic Reactions, Chem. Mater. 24 (2012) 4093–4099, doi:http://dx.doi.org/10.1021/cm302847r.
[31] T.F. Otero, J.G. Martinez, B. Zaifoglu, Using reactive artificial muscles to determine water exchange during reactions, Smart Mater. Struct. 22 (2013) 104019, doi:http://dx.doi.org/10.1088/0964-1726/22/10/104019.
[32] M. Fuchiwaki, J.G. Martinez, T.F. Otero, Polypyrrole Asymmetric Bilayer Artificial Muscle: Driven Reactions, Cooperative Actuation, and Osmotic Effects, Adv. Funct. Mater. 25 (2015) 1535–1541.
[33] L. Valero, J.G. Martinez, T.F. Otero, Creeping and structural effects in Faradaic artificial muscles, J. Solid State Electrochem. 19 (2015) 2683–2689, doi:http://dx.doi.org/10.1007/s10008-015-2775-1.
[34] T.F. Otero, J.G. Martinez, Artificial Muscles A Tool To Quantify Exchanged Solvent during Biomimetic Reactions, Chem. Mater. 24 (2012) 4093–4099, doi:http://dx.doi.org/10.1021/cm302847r.
[35] E. Smela, Conjugated Polymer Actuators for Biomedical Applications, Adv. Mater. 15 (2003) 481–494, doi:http://dx.doi.org/10.1002/adma.200390113.
[36] R. Kiefer, P.A. Kilmartin, G.A. Bowmaker, R.P. Cooney, J. Travas-Sejdic, Actuation of polypyrrole films in propylene carbonate electrolytes, Sens. Actuators B Chem. 125 (2007) 628–634, doi:http://dx.doi.org/10.1016/j.snb.2007.03.008.
[37] M. Fuchiwaki, T.F. Otero, Polypyrrole–para-phenolsulfonic acid/tape artificial muscle as a tool to clarify biomimetic driven reactions and ionic exchanges, J. Mater. Chem. B. 2 (2014) 1954–1965, doi:http://dx.doi.org/10.1039/C3TB21653E.
[38] L.V. Conzuelo, J. Arias-Pardilla, J.V. Cauich-Rodríguez, M.A. Smit, T.F. Otero, Sensing and Tactile Artificial Muscles from Reactive Materials, Sensors 10 (2010) 2638–2674, doi:http://dx.doi.org/10.3390/s100402638.
[39] M. Fuchiwaki, J.G. Martinez, T.F. Otero, Polypyrrole Asymmetric Bilayer Artificial Muscle: Driven Reactions, Cooperative Actuation, and Osmotic Effects, Adv Funct. Mater. 25 (2015) 1535–1541, doi:http://dx.doi.org/10.1002/adfm.201404061.
[40] B. Villeret, M. Nechtschein, Memory Effects in Conducting Polymers, Phys. Rev. Lett. 63 (1989) 1285–1287, doi:http://dx.doi.org/10.1103/PhysRevLett.63.1285.
[41] T. Sendai, H. Suematsu, K. Kaneto, Anisotropic Strain and Memory Effect in Electrochemomechanical Strain of Polypyrrole Films under High Tensile Stresses, Jpn. J. Appl. Phys. 48 (2009) 051506, doi:http://dx.doi.org/10.1143/JJAP.48.051506.
[42] M.A. Vorotyntsev, M. Skompska, E. Pousson, J. Goux, C. Moise, Memory effects in functionalized conducting polymer films: titanocene derivatized polypyrrole in contact with THF solutions, J. Electroanal. Chem. 552 (2003) 307–317, doi:http://dx.doi.org/10.1016/S0022-0728(03) 00038-X.
[43] J. Heinze, A. Rasche, The memory effect in solution, J. Solid State Electrochem. 10 (2006) 148–156, doi:http://dx.doi.org/10.1007/s10008-005-0056-0.
[44] T.F. Otero, M. Alfaro, V. Martinez, M.A. Perez, J.G. Martinez, Biomimetic Structural Electrochemistry from Conducting Polymers: Processes, Charges, and Energies Coulovoltammetric Results from Films on Metals Revisited, Adv. Funct. Mater. 23 (2013) 3929–3940, doi:http://dx.doi.org/10.1002/adfm.201203502.
[45] T.F. Otero, J.G. Martinez, Ionic exchanges, structural movements and driven reactions in conducting polymers from bending artificial muscles, Sens. Actuators B Chem. 199 (2014) 27–30, doi:http://dx.doi.org/10.1016/j.snb.2014.03.053.
[46] T.F. Otero, J.G. Martinez, M. Fuchiwaki, L. Valero, Structural Electrochemistry from Freestanding Polypyrrole Films: Full Hydrogen Inhibition from Aqueous Solutions, Adv. Funct. Mater. 24 (2014) 1265–1274, doi:http://dx.doi.org/10.1002/adfm.201302469.
[47] H. Grande, T.F. Otero, Intrinsic asymmetry, hysteresis, and conformational relaxation during redox switching in polypyrrole: A coulovoltametric study, J. Phys. Chem. B. 102 (1998) 7535–7540, doi:http://dx.doi.org/10.1021/jp9815356.
[48] T.F. Otero, J.M. Sansiñena, Bilayer dimensions and movement in artificial muscles, Bioelectrochem. Bioenerg. 42 (1997) 117–122, doi:http://dx.doi.org/10.1016/S0302-4598(96) 05112-4.
[49] T.F. Otero, M.T. Cortes, Artificial muscle: movement and position control, Chem. Commun. (2004) 284–285, doi:http://dx.doi.org/10.1039/b313132g.
[50] T.F. Otero, J.G. Martinez, Physical and chemical awareness from sensing polymeric artificial muscles. Experiments and modeling, Prog. Polym. Sci. 44 (2015) 62–78, doi:http://dx.doi.org/10.1016/j.progpolymsci.2014.09.002.
[51] J.G. Martinez, T.F. Otero, E.W.H. Jager, Effect of the Electrolyte Concentration and Substrate on Conducting Polymer Actuators, Langmuir 30 (2014) 3894–3904, doi:http://dx.doi.org/10.1021/la404353z.
[52] T.F. Otero, J.G. Martínez, B. Zaifoglu, Using reactive artificial muscles to determine water exchange during reactions, Smart Mater. Struct. 22 (2013) 104019, doi:http://dx.doi.org/10.1088/0964-1726/22/10/104019.
[53] L. Valero, T.F. Otero, J.G. Martínez, Exchanged Cations and Water during Reactions in Polypyrrole Macroions from Artificial Muscles, ChemPhysChem. 15 (2014) 293–301, doi:http://dx.doi.org/10.1002/cphc.201300878.